Available online at www.sciencedirect.com
SCIENCE DIRECT®
ELSEVIER
International Journal of Solids and Structures 42 (2005) 3045–3058
INTERNATIONAL JOURNAL OF SOLIDS and STRUCTURES
www.elsevier.com/locate/ijsolstr

Damping efficiency of the coating structure

Liming Yu, Yue Ma, Chungen Zhou, Huibin Xu *

School of Materials Science and Engineering, Beijing University of Aeronautics and Astronautics, Beijing, 100083, PR China

Received 28 October 2004
Available online 22 December 2004

Abstract

The damping efficiency of the coating system was discussed in this paper based on the Reuss model and Hashin–shtrickman equation. The theoretical results show that for a coating system, there exist an optimum thickness of the coating layer that make the coating structure obtain the best balance between the strength and the damping capacity. Enlarge the modulus difference between the coating layer and substrate will improve the damping and stiffness of the coating system simultaneously. The deviation between the theoretical predicted and experimental values on the dynamic modulus and damping capacity will be ameliorated while the stiffness difference between the coating layer and substrate increasing.

Keywords: Coating; Damping capacity; Dynamic modulus

1. Introduction

High damping materials are widely used to reduce vibration in aircraft, ship and other dynamic system. The benefit is longer service life of components, reductions in weight and in noise. Usually, the strength of materials or structure is characterized by complex modulus E^* under vibration environments

$$E^* = E' + \mathrm{i}E'' \tag{1}$$

in which E', E'' are storage modulus, loss modulus, respectively; and the module of E^* is written as $E = \sqrt{E'^2 + E''^2}$ generally. The loss factor $\tan\delta$ (the angle δ is the phase angle between stress and strain sinusoids) as a measure of damping is the ratio of the imaginary part to the real part of the complex modulus E^*, that is

* Corresponding author. Tel.: +86 108 231 5989; fax: +86 108 233 8200.
E-mail address: xuhb@buaa.edu.cn (H. Xu).

0020-7683/$ - see front matter
doi:10.1016/j.ijsolstr.2004.10.033

$$\tan\delta = \frac{E''}{E'} \tag{2}$$

It is very difficult to improve the damping capacity while ensuring the strength of materials or structure. However, in many structural applications it is desired to use materials that are not only stiff and strong, but also have the ability to damp mechanical vibrations. Since elastic modulus E measure the stiffness of the materials and $\tan\delta$ the damping, the product of the two $E\tan\delta$ is an useful figure of merit that combines both properties, and if there were a rational balance between E and $\tan\delta$, we would have no necessity to pursue a high level of damping capacity unilateral. Materials that combine high damping and high stiffness are not common (Brodt and Lakes, 1995; Lakes, 2002), for most of the existing materials $E\tan\delta \leqslant 0.6$ GPa, for example, the product $E\tan\delta$ of Al alloy, stainless steel, tungsten are 0.07 GPa, 0.2 GPa, 0.4 GPa, respectively. Developing a structural-functional materials which exhibit high stiffness and high damping is anticipated all along, and a possible method to realize this aim is to employ a multiple structure in which high damping coating and high stiffness substrate are combined (Cross et al., 1973; Buravalla et al., 2001; Yen and Shen, 2001). The damping efficiency of the coating system was discussed through theory and experimental in this paper.

2. Analysis

2.1. The damping of a coating composite structure

Fig. 1 is the sketch of the coating system under vibrational load. The main source of high damping performance of such structure may be as follows:

(1) *Non-affined local strain field effect*. The modulus of the coating layer and substrate are usually unequal, so there are non-affined deformation field in and near the interface under vibration load (Chen and Lakes, 1993a,b; Gibiansky and Lakes, 1993). This local deformation will cause two effects: first, the non-affined deformation will take a disturbance effect in time domain, and enlarge the phase angle δ between stress and strain, hence improve the structure's damping capability; second, the high local deformation in and near the interface may be much more than that of the whole coating structure, which will contribute to the increasing of the energy-storing effect, and increase the storage modulus of the coating system. The non-affined deformation effect is not a special property of the coating structure, but some composite damping materials (such as MMC damping materials, Zhang et al., 1994) and particle- or fiber-reinforced composites (Chandra et al., 2002) attain high stiffness and high damping performance through the same effects.
(2) *Constrained damping effect*. The coating layer will induce a constrained damping structure (Magdenkov, 1996).

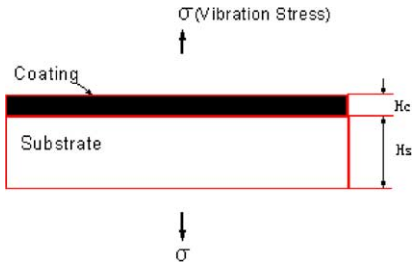

Fig. 1. The sketch of a coating structure under vibration loaded.

(3) *Interface effect*. Coating will induce new interface (Nelson and Hancock, 1978); in addition, some special structure of the coating (for example, thermally-sprayed coating usually have porosities ranging from a few percent to about 20%, McPherson, 1989) may be the high damping source under vibrational load.
(4) *Intrinsic damping*. There is intrinsic damping of the coating and substrate materials. Unfortunately, the intrinsic damping capacity of the most structural materials is very poor.

For a coating structure as Fig. 1, the effective damping $\tan\delta$ can be approximate calculated as follows (Lakes, 2002):

$$\tan\delta \approx \frac{3E'_c \tan\delta_c H_c}{E'_s H_s} \tag{3}$$

in which E'_c, E'_s, H_c, H_s are the storage modulus and thickness of coating layer and substrate, respectively, and $\tan\delta_c$ is the loss factor of the coating layer. Eq. (3) means that if we merely consider the damping capability, the effective damping $\tan\delta$ of the coating structure will be linear with the thickness of the coating H_c. But an oversize H_c will take a disadvantageous influence on the strength of the whole coating structure (Wu et al., 1989) and lower the performance of $E\tan\delta$. This indicates that there may exist an optimal geometry size of the coating H_c, which makes the product $E\tan\delta$ attain the maximum level.

2.2. Theory

In terms of the materials morphologies and loaded conditions, the coating structure is very closed to the Reuss composite (Fig. 2) (Hwang and Hwang, 1999). During our study we consider the Reuss model since it is simple and is realizable physically. A more strictly bounded stiffness value of multi-phase composite structure was processed by Hashin–Shtrikman formula (Hashin and Shtrikman, 1963), so this theory is also considered for the sake of comparison.

In the Reuss structure, two different phases are aligned perpendicular to the direction of the external load so that they experience the same stress. The Reuss formula is widely used to predict the mechanical property of laminate composite materials and structure. Based on the correspondence principle (Hashin, 1970), the generalized Reuss formula can be expressed

$$\frac{1}{E^*} = \sum \frac{V_i}{E_i^*} \tag{4}$$

in which E^*, E_i^* refer to the dynamic modulus of the whole composite, the dynamic modulus of the components, and V_i refers to the volume fraction of the components with $\sum V_i = 1$ (Fig. 2(a)). For a coating structure (Fig. 2(b)), the Reuss formula can be simplified as follows:

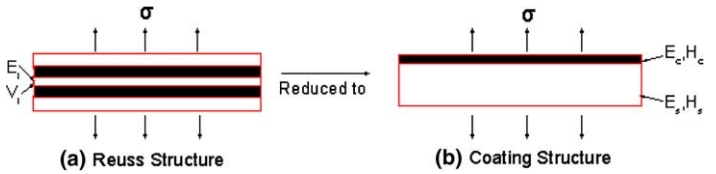

Fig. 2. The Reuss structure and the coating structure. The materials morphologies of two structures are laminate distributing, and each phase experiences the same stress under perpendicular vibration loaded.

$$\frac{1}{E^*} = \frac{H_s}{E_s^*} + \frac{H_c}{E_c^*} \tag{5}$$

By substituting $E^* = E' + iE''$ into Eq. (5) and separating the real and imaginary part of E^*, modulus E and loss factor $\tan\delta$ of the coating structure are obtained

$$E = \frac{E_c/(1-H_c)}{\left((E_c/E_s)^2 + (H_c/(1-H_c))^2 + (E_c/E_s)(H_c/(1-H_c))\frac{2(1+\tan\delta_s\tan\delta_c)}{\sqrt{(1+\tan\delta_s^2)(1+\tan\delta_c^2)}}\right)^{1/2}} \tag{6}$$

$$\tan\delta = \frac{(E_c/E_s)\tan\delta_s\sqrt{1+\tan\delta_c^2} + (H_c/(1-H_c))\tan\delta_c\sqrt{1+\tan\delta_s^2}}{(E_c/E_s)\sqrt{1+\tan\delta_c^2} + (H_c/(1-H_c))\sqrt{1+\tan\delta_s^2}} \tag{7}$$

Eq. (7) means that for a given coating system, the structure damping $\tan\delta$ depend on the ratio of the coating and substrate's modulus E_c/E_s and the thickness fraction of the coating layer H_c, that is

$$\tan\delta = f\left(\frac{E_c}{E_s}, H_c\right) \tag{8}$$

The above-motioned discussion is based on the transverse loading of the coating's vibration model. Another common vibrational model is the shear vibration, which is not considered in this paper. For laminate morphology materials, some researcher thought that the damping capacity of two vibration models is very similar (Vantomme, 1995; Chen et al., 2002).

Different to Reuss model, the influence of Poisson's ratio υ is taken into account in Hashin–Shtrikman method. The shear modulus of the hierarchical structure is processed by the H–S formula. The performance of the composite layer was discussed based on the H–S theory by Francfort and Murat (1986). Applied for coating system, the shear modulus G^* can be given as

$$G^* = G_c^* + \frac{H_s}{\frac{1}{G_s^*-G_c^*} + \frac{6(K_c^*+2G_c^*)H_c}{5(3K_c^*+4G_c^*)G_c^*}} \tag{9}$$

in which G_s^*, K_s^* and G_c^*, K_c^* are the shear modulus, bulk modulus of substrate and coating, respectively. The relationship between these pairs are given by the formulas

$$G^* = \frac{3K^*(1-2\upsilon)}{2(1+\upsilon)} \tag{10}$$

$$E^* = 2G^*(1+\upsilon) \tag{11}$$

Substituting Eqs. (10) and (11) into Eq. (9), we obtain

$$E^* = \frac{E_c^*(1+\upsilon)}{1+\upsilon_c} + \frac{H_s(1+\upsilon)}{\frac{(1+\upsilon_s)(1+\upsilon_c)}{(1+\upsilon_c)E_s^*-(1+\upsilon_s)E_c^*} + \frac{[2(1+\upsilon_c)^2+6(1+\upsilon_c)(1-2\upsilon_c)]H_c}{[5(1+\upsilon_c)+10(1-2\upsilon_c)]E_c^*}} \tag{12}$$

in which υ_c, υ_s are Poisson's ratio of the coating, substrate, respectively; υ refer to the coating system's Poisson's ratio and it can be written as

$$\upsilon = H_c\upsilon_c + H_s\upsilon_s \tag{13}$$

Separating the real and imaginary part of E^*, we can obtain the coating structure's Young's modulus E and loss factor $\tan\delta$ based on the H–S theory. As E and $\tan\delta$ are too complicated to write explicitly in this case, it is expedient to graphically display the computed numerical values.

3. Numerical examples

3.1. The Reuss model results

3.1.1. The influence of the E_c and E_s

Some numerical examples, based on the Reuss model, are presented here for a coating structure. We consider such kinds of substrates with modulus $E_s = 70 \sim 400$ GPa, and the loss factor $\tan\delta_s = 0.001$. The strength and the damping capacity of the most metal structural materials (such as Al alloy, Ti alloy, stainless steel, tungsten, etc) are within this range, and the product $E_s \tan\delta_s$ of these substrates are $0.07 \sim 0.4$ GPa (Lakes, 2002; Vaidya et al., 1995). Supposing the modulus E_c and the damping $\tan\delta_c$ of the coating layer are 30 GPa and 0.1 respectively (some high damping metal, such as gray cast iron, InSn alloy and some high-loss viscoelastic materials have such performance, Cook and Lakes, 1995), the results are plotted as $\tan\delta - (E_c/E_s) - H_c$ map, $E - (E_c/E_s) - H_c$ map and $E\tan\delta - (E_c/E_s) - H_c$ map as shown in Fig. 3(a)–(c), respectively.

The Y-axis in Fig. 3 is E_c/E_s, which reflects the stiffness difference between the coating layer and substrate. Fig. 3(a) and (b) are the relationship between the modulus E and the damping $\tan\delta$ of the coating system and the thickness fraction of the coating H_c. It is obvious that the coating structure's modulus and damping capacity change in the opposite direction while increasing H_c. But on the other hand, when the ratio E_c/E_s approaches zero, which means the stiffness difference between the coating layer and substrate is increasing, the modulus and the damping capacity of the coating structure will increase simultaneously. That is to say, when the geometry size of a coating structure is fixed, enlarging the stiffness difference

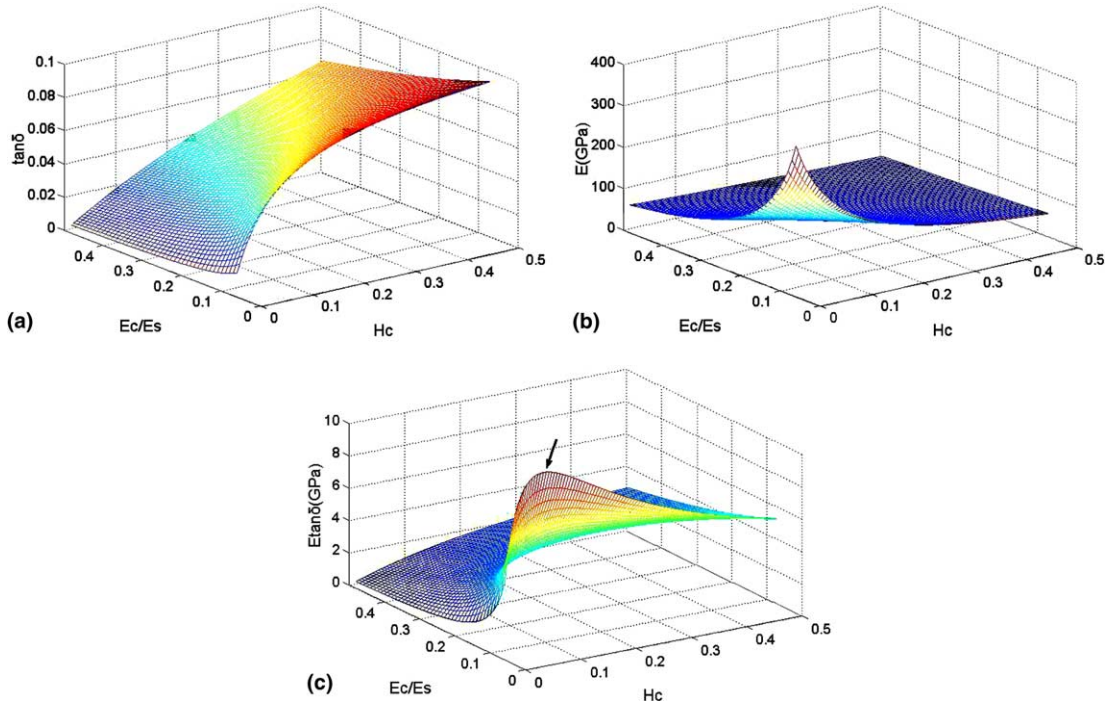

Fig. 3. The influence of the ratio E_c/E_s on the damping efficiency of a coating structure (based on the Reuss model). The modulus and damping of substrate, coating layer are 70–400 GPa and 0.001, 30 GPa and 0.1, respectively. (a) $\tan\delta - (E_c/E_s) - H_c$ plot, (b) $E - (E_c/E_s) - H_c$ plot and (c) $E\tan\delta - (E_c/E_s) - H_c$ plot. The product $E\tan\delta$ has a maximum value (denoted by the arrow in Fig. 3(c)).

between the coating and substrate will improve the strength and damping performance of the coated sample at the same time.

The relationship between product $E\tan\delta$ and H_c is shown in Fig. 3(c). With a given E_c/E_s value, the product $E\tan\delta$ has a maximum value (denoted by the arrow in Fig. 3(c)), which increase while E_c/E_s tends toward zero. The existence of the maximum value of $E\tan\delta$ is very importance to the design of damping coating, especially when the strength and the damping of a coating structure need to be considered simultaneously.

Eq. (7) shows that, when $(E_c/E_s) \to 0$ (which means the difference of the modulus of the coating and substrate is very notable), the damping of the coating structure $\tan\delta$ will trend to $\tan\delta_c$, the higher damping phase in the coating system. Such result shows that, based on the Reuss model, the theoretical damping of the coating structure will trend to that of the highest damping component in the coating system while the stiffness difference of the coating layer and substrate increasing. But there are some differences between the theoretical predicted and experimental, and it will be discussed later.

3.1.2. The influence of the $\tan\delta_c$ and $\tan\delta_s$

Similar to E_c/E_s, another influence factor was the ratio $\tan\delta_c/\tan\delta_s$. Eq. (6) and (7) can be rewritten as

$$E = \frac{E_c/(1-H_c)}{\left((E_c/E_s)^2 + (H_c/(1-H_c))^2 + (E_c/E_s)(H_c/(1-H_c))\frac{2(t+1/\tan\delta_s^2)}{\sqrt{t^2(1+1/\tan\delta_s^2)+\left(1/\tan\delta_s^2+1/\tan\delta_s^4\right)}}\right)^{1/2}} \tag{14}$$

$$\tan\delta = \frac{\tan\delta_s(E_c/E_s)\sqrt{t^2+1/\tan\delta_s^2} + t(H_c/(1-H_c))\sqrt{1+\tan\delta_s^2}}{(E_c/E_S)\sqrt{t^2+1/\tan\delta_s^2} + (H_c/(1-H_c))\sqrt{1+1/\tan\delta_s^2}} \tag{15}$$

where $t = \tan\delta_c/\tan\delta_s$.

The influence of the ratio $\tan\delta_c/\tan\delta_s$ and the coating layer thickness H_c were shown in Fig. 4 (based on Eqs. (14) and (15)), in which the coating system performance were supposed: $E_s = 200$ GPa, $\tan\delta_s = 0.001$ and $E_c = 30$ GPa, $\tan\delta_c = 0.1$–0.001. It can be seen that, when the modulus of the substrate and the coating layer were given, the damping capacity of the coating system $\tan\delta$ increased along with the increasing of the ratio $\tan\delta_c/\tan\delta_s$ (Fig. 4(a)). However the ratio $\tan\delta_c/\tan\delta_s$ has no influence on the modulus of the coating structure E (Fig. 4(b)). Fig. 4(c) shown that, despite the ratio $\tan\delta_c/\tan\delta_s$ distributed in a wide range (from 1 to 100), its influence on the product $E\tan\delta$ was relatively limited.

It also can be found in Fig. 4(c) that, with a given $\tan\delta_c/\tan\delta_s$ value, there exist an optimum coating thickness H_c which make the product $E\tan\delta$ obtain the maximum value (similar to the Fig. 3(c)). However, an exceptional case was $(\tan\delta_c/\tan\delta_s) = 1$ (see the arrow in Fig. 4(c)). In this case, $E\tan\delta$ has no maximum value. The optimum coating thickness H_c was discussed in the following section.

3.1.3. The optimum coating thickness H_c

Figs. 3(c) and 4(c) shows that, for a coating system, an optimum coating layer thickness H_c would exist. But one case was exceptional, i.e. when the coating layer and the substrate have the same damping capacity $(\tan\delta_c = \tan\delta_s)$. The partial differential principle was utilized to estimate the existence of the optimum thickness H_c in this section. Two kinds of cases were discussed as follows:

Case I: When $\tan\delta_c = \tan\delta_s = \tan\delta'$

In this case, Eqs. (6) and (7) can be rewritten as

$$E = \frac{E_c/(1-H_c)}{(E_c/E_s) + (H_c/(1-H_c))} \tag{16}$$

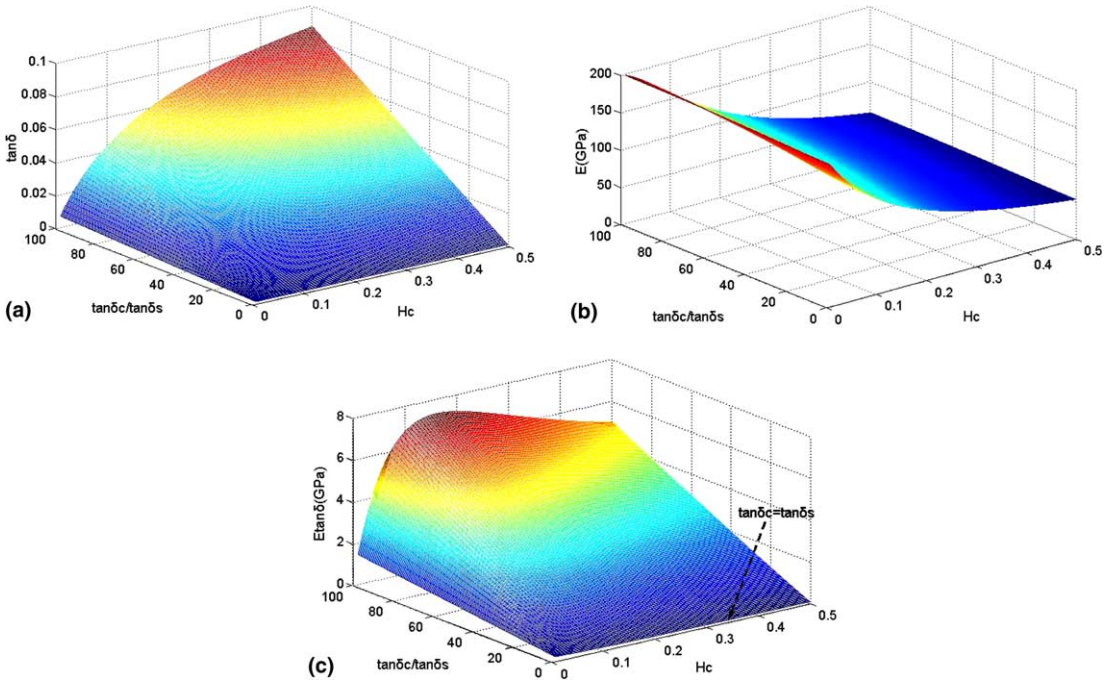

Fig. 4. The influence of the ratio $\tan\delta_c/\tan\delta_s$ on the damping efficiency of a coating structure. The coating system performance were supposed: $E_s = 200$ GPa, $\tan\delta_s = 0.001$ and $E_c = 30$ GPa, $\tan\delta_c = 0.1 \sim 0.001$. (a) $\tan\delta - (\tan\delta_c/\tan\delta_s) - H_c$ plot, (b) $E - (\tan\delta_c/\tan\delta_s) - H_c$ plot and (c) $E\tan\delta - (\tan\delta/\tan\delta_S) - H_c$ plot. The product $E\tan\delta$ has a maximum value. But $(\tan\delta_c/\tan\delta_s) = 1$ was a exceptional case (see the arrow in (c)).

$$\tan\delta = \tan\delta' \tag{17}$$

Using the partial differential principle, one obtains

$$\frac{\partial(E\tan\delta)}{\partial H_c} = E_c E_s \tan\delta' \frac{(E_c - E_s)}{[E_c + (E_s - E_c)H_c]^2} \tag{18}$$

When the substrate and the coating layer have different modulus, i.e., $E_c \neq E_s$, we have

$$\frac{\partial(E\tan\delta)}{\partial H_c} \neq 0 \tag{19}$$

Eq. (19) means that the product $E\tan\delta$ was a monotone function of the thickness H_c. Thus the optimum thickness H_c did not exist. This case was pointed out by the arrow in Fig. 4(c).

A specific case must be considered here, i.e., when $E_c = E_s = E'$. In this case, Eqs. (6) and (7) became

$$E = E', \quad \tan\delta = \tan\delta' \tag{20}$$

Then we have

$$E\tan\delta = E'\tan\delta' \tag{21}$$

This shown that, when $\tan\delta_c = \tan\delta_s$ and $E_c = E_s$, the value of the product $E\tan\delta$ was independent of the coating thickness H_c. Thus the optimum thickness H_c did not exist too.

In fact, even though the damping capacity of the substrate and the coating layer were very close to each other, the damping of the coated sample has a notable improvement compared to the substrate (Yu et al., 2005). The physical mechanism of the coating structure damping deserves deeper research.

Case II: When $\tan\delta_c \neq \tan\delta_s$

Usually, the damping capacity of the coating layer and the substrate are not equal, i.e. $\tan\delta_c \neq \tan\delta_s$. In this case, employing Eqs. (6) and (7), the partial differential $\frac{\partial(E\tan\delta)}{\partial H_c}$ can be obtained (analogous to Eq. (18))

$$\frac{\partial(E\tan\delta)}{\partial H_c} = \frac{E_c(C_1C_4 - C_2C_3)}{(C_3H_c + C_4)^2[AH_c^2 + BH_c + (E_c/E_S)^2]^{1/2}} - \frac{E_c(2AH_c + B)(C_1H_c + C_2)}{2(C_3H_c + C_4)[AH_c^2 + BH_c + (E_c/E_s)^2]^{3/2}} \tag{22}$$

where

$$A = \left(\frac{E_c + E_s}{E_c}\right)^2 - \frac{2E_c(1 + \tan\delta_c\tan\delta_s)}{E_s[(1 + \tan\delta_s^2)(1 + \tan\delta_c^2)]^{1/2}},$$

$$B = \frac{2E_c(1 + \tan\delta_c\tan\delta_s)}{E_s[(1 + \tan\delta_s^2)(1 + \tan\delta_c^2)]^{1/2}} - 2\left(\frac{E_c}{E_s}\right)^2,$$

$$C_1 = \tan\delta_c(1 + \tan\delta_s^2)^{1/2} - \tan\delta_s(E_c/E_s)(1 + \tan\delta_c^2)^{1/2},$$

$$C_2 = \tan\delta_s(E_c/E_s)(1 + \tan\delta_c^2)^{1/2},$$

$$C_3 = (1 + \tan\delta_s^2)^{1/2} - (E_c/E_s)(1 + \tan\delta_c^2)^{1/2},$$

$$C_4 = (E_c/E_s)(1 + \tan\delta_c^2)^{1/2},$$

Notice that A, B, C_1, C_2, C_3 and C_4 were independent of the coating thickness H_c. The product $E\tan\delta$ would obtain the maximum value when $\frac{\partial(E\tan\delta)}{\partial H_c} = 0$, i.e.,

$$\frac{E_c(C_1C_4 - C_2C_3)}{(C_3H_c + C_4)^2[AH_c^2 + BH_c(E_c/E_s)^2]^{1/2}} - \frac{E_c(2AH_c + B)(C_1H_c + C_2)}{2(C_3H_c + C_4)[AH_c^2 + BH_c + (E_c/E_s)^2]^{3/2}} = 0 \tag{23}$$

The solution of Eq. (23) was the optimum coating thickness H_c. Let us examine a numerical example case: a coating system having $E_s = 200$ GPa, $\tan\delta_s = 0.001$ and $E_c = 30$ GPa, $\tan\delta_c = 0.01$. In this case, the solution of Eq. (23) was $H_c = 0.147$, and the maximum value of the $E\tan\delta$ was 0.634 GPa. This fact is also illustrated in Fig. 5.

3.2. The predicted difference between the Reuss model and the H–S equation

Fig. 6 shows the difference of the numerical result between Reuss mode and H–S method. In this example, the performance of the coating layer and the substrate are assumed to be as: $E_c = 30$ GPa, $\tan\delta_c = 0.1$; $E_s = 200$ GPa, $\tan\delta_s = 0.001$. The change in relation between $\tan\delta$, E of the coating system and H_c based on two models are shown in Fig. 6(a) and (b). It can be find that the damping $\tan\delta$ based on H–S equation is lower than the calculate results of the Reuss model, yet the predict results of E based on two method are opposite to the $\tan\delta$. Fig. 6(c) and (d) show that the discrepancy of the performance $E\tan\delta$ of coating structure based on two methods is rather small. Though the maximum value of $E\tan\delta$ appears on difference H_c, the tendencies of two ways are very similar.

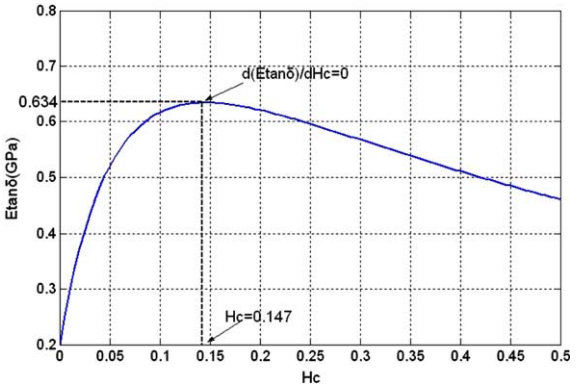

Fig. 5. A numerical solution of the optimum coating thickness H_c. The coating system having $E_s = 200$ GPa, $\tan\delta_s = 0.001$ and $E_c = 30$ GPa, $\tan\delta_c = 0.01$. In this case, $\tan\delta_c \neq \tan\delta_s$, and the optimum $H_c = 0.147$.

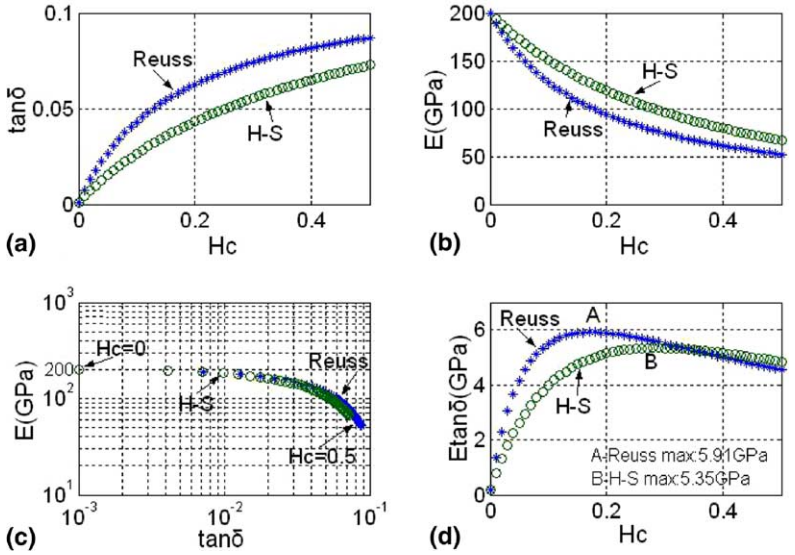

Fig. 6. The predicted difference of damping efficiency between Reuss model and H–S equation. The performance of the coating system are: $E_c = 30$ GPa, $\tan\delta_c = 0.1$; $E_s = 200$ GPa, $\tan\delta_s = 0.001$. (a) $\tan\delta - H_c$ curve, (b) $E - H_c$ curve and (c) $E - \tan\delta$ map; (d) $E\tan\delta - H_c$ curve.

4. Experimental results

In this paper, the coatings were prepared by atmosphere plasma-sprayed (APS) method. The substrate materials were 1Cr18Ni9Ti stainless steel, 1Cr13 stainless steel and DZ125 high-temperature alloy, and the coatings layer were NiCrAlY metal and Al_2O_3 ceramic coating. The thickness of substrate, coating layer were 950–1000 μm, 110–150 μm, respectively. The spraying technical parameters were listed in Table 1.

The dynamic modulus E and the damping $\tan\delta$ were measured by dynamic mechanical thermal analyzer (DMTA), in which three-point bending method was applied. The dynamic storage modulus (E') and loss modulus (E'') can be simultaneously measured by DMTA, and the modulus E and the damping $\tan\delta$

Table 1
The plasma spray conditions of NiCrAlY coating and Al_2O_3 coating

Voltage (V)	Current (A)	Argon gas (l/min)	Hydrogen gas (l/min)	Powder feed rate (g/min)
55–60	550–580	60	30	20

Table 2
The performance of the coating system components

	Al_2O_3	NiCrAlY	1Cr18Ni9Ti	1Cr13	DZ125
E (GPa)	64	117	202	188	221
$\tan\delta$ ($\times10^{-3}$)	0.1	3.01	4.83	11	4.73

Table 3
The performance of the coated sample

Substrate + coating	DZ125 + Al_2O_3	1Cr18Ni9Ti + Al_2O_3	1Cr13 + NiCrAlY
E (GPa)	131	119	107
$\tan\delta$ ($\times10^{-3}$)	4	5.32	27
$E\tan\delta$ (GPa)	0.53	0.63	2.89

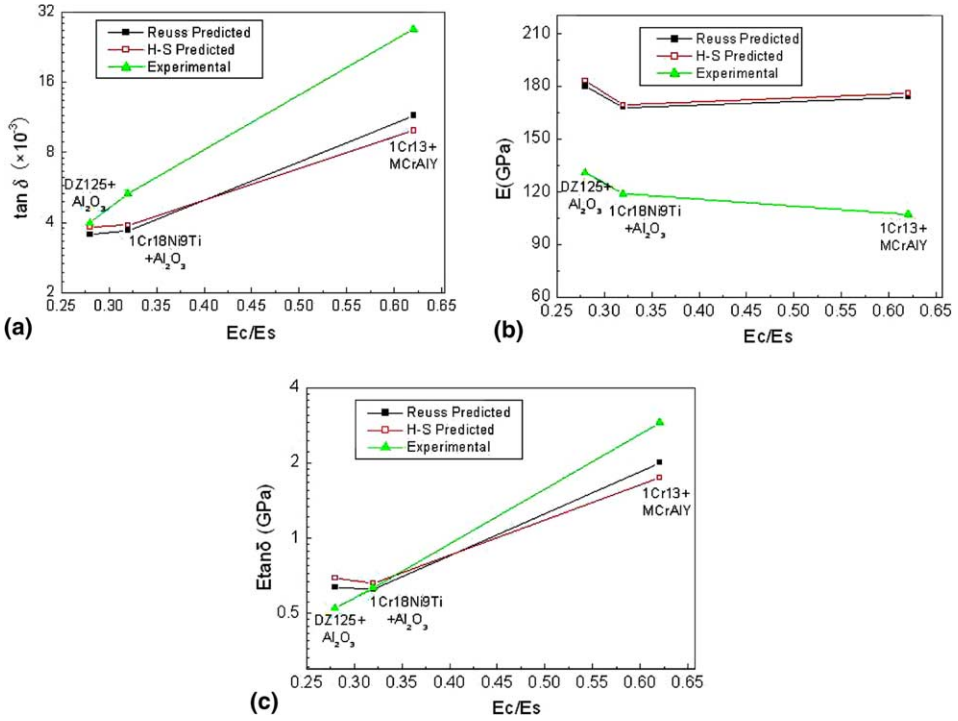

Fig. 7. The difference of damping efficiency between theory predicted and experimental. The substrate materials are 1Cr18Ni9Ti, 1Cr13 stainless steel and GH30 high-temperature alloy, and the coatings are NiCrAlY metal coating and Al_2O_3 ceramic coating. The thickness of substrate, coating layer are 950–1000 μm, 110–150 μm, respectively. The deviation between the theory predicted and experimental value on the damping capacity and dynamic modulus were ameliorated while E_c/E_s tends to zero in (a) and (b) (that means the stiffness difference between the coating layer and substrate is increasing). (a) The difference of $\tan\delta$ between theory predicted and experimental. (b) The difference of E between theory predicted and experimental. (c) The difference of $E\tan\delta$ between theory predicted and experimental.

can be calculated. The measured strain, frequency and temperature were 0.04%, 10 Hz and room temperature, respectively.

The test results of the coating system components were listed in Table 2 (the parameter of Al_2O_3 coating layer was measured by Vaidya et al. (1995)). And the performance of the whole coated sample are listed in Table 3. The product $E\tan\delta$ of three coating systems were 0.53, 0.63 and 2.89 GPa, respectively, and have approached or exceeded the value of 0.6 GPa.

The difference between theoretical predicted and experimental results of the damping $\tan\delta$, modulus E and product $E\tan\delta$ of three coated sample were show in Fig. 7(a)–(c) respectively (the Poisson's ratio υ is thought to be 0.3 approximately in H–S method). Fig. 7(a) shows that the experimental values of the damping $\tan\delta$ are always higher than theoretical predicted one. The theoretical results are approaching the experimental value as the stiffness difference between the coating and substrate increasing (i.e. when $(E_c/E_s) \to 0$). And this tendency is more distinct while applying H–S model, the reason may be that H–S model has considered the influence of the Poisson's ratio υ, so it could more accurately reflect the influence of the non-affined deformation field within and near the interface under vibrational load. These results also mean that the Reuss model and H–S method could be more suitable to predict the damping of the coating system when the modulus difference between the coating layer and substrate is very notable. Fig. 7(b) shows that the theoretically predicted value is higher than the experimental. Fig. 7(c) shows that the theory predicted of $E\tan\delta$ by two methods resemble in the experimental value.

5. Discussion

The inhomogeneous degree of the local strain field, which exists within and near the interface, was depended on the stiffness difference between the coating layer and substrate (i.e. E_c/E_s) under a vibrational environment. When the stiffness difference become greater, which means E_c/E_s tends to zero, the impact of non-affined local strain filed effects would become stronger correspondingly, so a more accurate predicted results by the Reuss and H–S theory could be obtained (Fig. 7(a) and (b)).

As can be seen (Figs. 3(c) and 4(c)) that, for a coating system, the maximum value of produce $E\tan\delta$ could be obtained when the coating layer H_c is optimum. The relationship between the maximum of $E\tan\delta$ and the ratio E_c/E_s based on the Reuss equation is shown in Fig. 8. As contrasted, the curve of

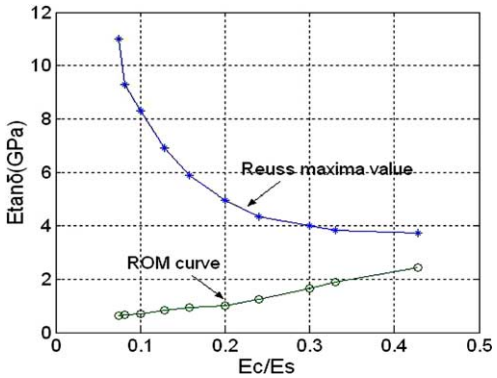

Fig. 8. The influence of E_c/E_s on the maximum value of $E\tan\delta$ base on the Reuss model and ROM. The distance of two curves is increasing with the direction of $(E_c/E_s) \to 0$.

$E\tan\delta - (E_c/E_s)$ based on rule of mixture (ROM) (Wolfenden and Wolla, 1991) of the component's performance is also shown in Fig. 8. In general, the ROM equation can be written as Eq. (24)

$$E\tan\delta = H_s E_s \tan\delta_s + H_c E_c \tan\delta_c \tag{24}$$

In Eq. (24), the coating layer thickness H_c was the optimum value which was decided by the Reuss Model. The maximum value of $E\tan\delta$ based on the Reuss model is far larger than the calculated value based on the ROM, and with the stiffness difference of the coating layer and substrate increasing ($(E_c/E_s) \to 0$), the distance of two curve is correspondingly increasing too. This is a rational result, because the more stiffness difference between the coating and substrate, the more fierceness interaction effective on the interface. It is obvious that a simple linear adding of materials performance (i.e. ROM) cannot reflect such tendency.

Based on Reuss model, the influence effects of the ratio E_c/E_s and the ratio $\tan\delta_c/\tan\delta_s$ to the coating system are shown in Fig. 9. We consider such kinds of coating system: $E_s = 200$ GPa, $\tan\delta_s = 0.001$ (a typical stainless steel material), and $E_c = 30$ GPa, $\tan\delta_c = 0.1$. The $E - \tan\delta$ map and $E\tan\delta - H_c$ plot were according to Curve 1 in Fig. 9(a) and (b) respectively, and in this case, $(E_c/E_s) = 0.15$ and $(\tan\delta_c/\tan\delta_s) = 100$. Curve 2 shows the effects of increasing the stiffness of substrate E_s from 200 to 400 GPa while the damping capacity of each components fixed, i.e. $E_c/E_s = 0.075$ and $\tan\delta_c/\tan\delta_s = 100$; Curve 3 show the effect of increasing the damping of the substrate ($\tan\delta_s$) from 0.001 to 0.01 while the modulus of the coating system keep fixed, i.e. $E_c/E_s = 0.15$ and $\tan\delta_c/\tan\delta_s = 10$.

It is obviously that on the aspect of improving the integrated performance $E\tan\delta$ of the coating system, increasing the stiffness difference between the coating layer and substrate is far more effective than increasing the damping capability of the components only. The increasing of stiffness difference will lead to a more drastic non-affined deformation field within and near the interface; moreover, improving the modulus of substrate is more feasible than improving the damping capacity of it, as the gain of damping performance of the materials always accompanies the loss of its strength.

The theoretical structure damping of the coated sample that predicted by Reuss model and H–S method will never exceed the highest damping of the component, but this do not comply with the experimental results (Tables 2 and 3). In Reuss model and H–S equation, the interface condition in coating system are idealized; furthermore, some structural factors (such as the porosity which widely exist in plasma sprayed coating) and some energy factors (such as residual stress, surface energy, etc.) in the actual coating system will influence the damping efficiency also. Fig. 10 shows a typical SEM image for NiCrAlY plasma coating, where the internal ''interfaces'', including the macro-interface between the coating layer and sub-

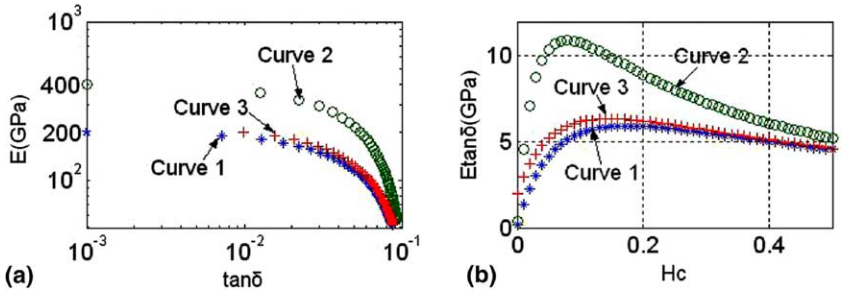

Fig. 9. The influence effects on the coating's damping efficiency. (a) E-tan δ map; (b)Etan δ-H_c curve. It can be seen that the ratio E_c/E_s has a far more notable influence effects on the product $E\tan\delta$ of the coating system than the effects of the components damping capacity. Curve 1: $E_c = 30$ GPa, $\tan\delta_c = 0.1$; $E_s = 200$ GPa, $\tan\delta_s = 0.001$; $(E_c/E_s) = 0.15$, $(\tan\delta_c/\tan\delta_s) = 100$. Curve 2: $E_c = 30$ GPa, $\tan\delta_c = 0.1$; $E_s = 400$ GPa, $\tan\delta_s = 0.001$; $(E_c/E_s) = 0.075$, $(\tan\delta_c/\tan\delta_s) = 100$. Curve 3: $E_c = 30$ GPa, $\tan\delta_c = 0.1$; $E_s = 200$ GPa, $\tan\delta_s = 0.01$; $(E_c/E_s) = 0.15$, $(\tan\delta_c/\tan\delta_s) = 10$.

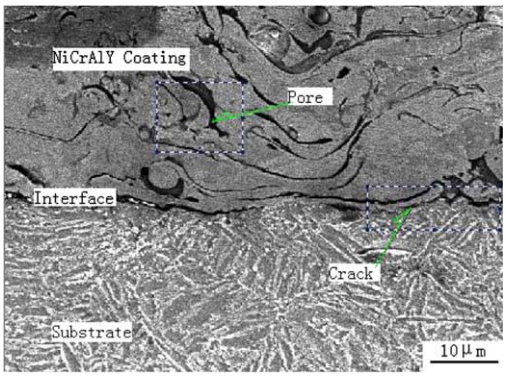

Fig. 10. SEM image of the NiCrAlY coating. The internal interfaces and porosity can be seen.

strate, lamellar interface in the coating layer etc., and porosity can be seen. All these structural may be the high damping source under vibrational load, for example, a conjugation defects in the interface may result in local interface slip, and combine with viscous damping (Nelson and Hancock, 1978). On the other hand, the non-idealization interface conjugation condition and structure defects (such as porosity) in the coating layer may impair the strength of the coating structure. This may be the reason that the experimental damping capacity of the coated sample is higher than theoretical predicted while the experimental dynamic modulus is lower than the theoretical value.

6. Conclusions

(1) The theoretic results based on the Reuss model and Hashin–Shtrikman equation show that for a coated beam structure, there exist an optimum thickness of the coating layer H_c that make the product $E\tan\delta$ of the coating system obtain the maximum value provided that the damping capacity of the coating layer and the substrate are not equal. Enlarge the modulus difference between the coating and substrate will increase the non-affined degree of the local deformation field in and near the interface, and improve the damping and strength of the coating structure. The ratio E_c/E_s has a far more notable influence effects on the product $E\tan\delta$ of the coating system than the effects of the components damping capacity.

(2) The interface condition is thought to be idealized, and the influences of actual structure factors and energy factors are not considered in the Reuss mode and H–S method, so there are some differences between the theoretical value and the experimental results. The experimental damping is higher than the theoretical, and the disparity will be ameliorated while the modulus difference between the coating and substrate increasing. The experimental value of modulus is smaller than the theoretical value. The experimental value of $E\tan\delta$ and theoretical prediction are close to each other.

References

Brodt, M., Lakes, R.S., 1995. Composite materials which exhibit high stiffness and high viscoelastic damping. J. Compos. Mater. 29 (14), 1823–1833.

Buravalla, V.R., Remillat, C., Tomlinson, G.R. et al., 2001. Advances in damping materials and technology. Smart Mater. Bull. 8, 10–13.

Chandra, R., Singh, S.P., Gupta, K., 2002. Micromechanical damping models for fiber-reinforced composites: a comparative study. Composites: Part A 33, 787–796.

Chen, C.P., Lakes, R.S., 1993a. Viscoelastic behaviour of composite materials with convention- or negative Poisson's-ratio foam as one phase. J. Mater. Sci. 28, 4288–4298.

Chen, C.P., Lakes, R.S., 1993b. Analysis of high-loss viscoelastic composites. J. Mater. Sci. 28, 4299–4304.

Chen, Z.R., Yu, S.W., Feng, X.Q. et al., 2002. A micromechanics model for estimating the effective thermoelastic properties of layered media. Compos. Sci. Technol. 62, 441–449.

Cook, L.S., Lakes, R.S., 1995. Damping at high homologous temperature in pure Cd, In, Pb, and Sn. Scripta Metall. Mater. 32 (5), 773–777.

Cross, K.R., Lull, W.R., Newman, R.L., 1973. Potential of graded coatings in vibration damping. J. Aircraft 10 (11), 689–691.

Francfort, G.A., Murat, F., 1986. Homogenization and optimal bounds in linear elasticity. Arch. Rational. Mech. Anal. 94, 307–334.

Gibiansky, L.V., Lakes, R.S., 1993. Bounds on the complex bulk modulus of a two-phase viscoelastic composite with arbitrary fractions of the components. Mech. Mater. 16, 317–331.

Hashin, Z., 1970. Complex modulus of viscoelastic composites: I. General theory and application to particulate composites. Int. J. Solids Struct. 6, 539–552.

Hashin, Z., Shtrikman, S., 1963. A variational approach to the elastic behaviour of multiphase materials. J. Mech. Phys. Solids 11, 127–140.

Hwang, K.C., Hwang, Y.G., 1999. Constitutive Theory of Solid. Tsinghua University Press, pp. 135–143.

Lakes, R.S., 2002. High damping composite materials: effect of structural hierarchy. J. Compos. Mater. 36 (03), 287–297.

Magdenkov, V.A., 1996. The new type of constrained vibration-damping coating. J. Low Frequency Noise Vib. 15 (3), 107–113.

McPherson, R., 1989. A review of microstructure and properties of plasma sprayed ceramic coatings. Surf. Coat. Technol. 39/40, 173–181.

Nelson, D.J., Hancock, J.W., 1978. Interfacial slip and damping in fibre-reinforced composites. J. Mater. Sci. 13, 2429–2440.

Vaidya, R.U., Zurek, A.K., Wolfenden, A. et al., 1995. Effect of plasma-sprayed alumina on the strength, elastic modulus, and damping of Ti–25Al–10Nb–3V–1Mo Intermetallic. J. Mater. Eng. Perform. 4 (3), 252–258.

Vantomme, J., 1995. A parametric study of materials damping in fiber-reinforced plastics. Composites 26, 147–153.

Wolfenden, A., Wolla, J.M., 1991. Dynamic Mechanical Properties in MMC[M]. Academic Press Inc, San Diego, p. 287.

Wu, B.C., Chang, E., Chang, S.F., Tu, D., 1989. Degradation mechanisms of YSZ thermal barrier coating. J. Am. Ceram. Soc 72 (2), 212–218.

Yen, H.Y., Shen, M.H., 2001. Passive vibration suppression of beams and bland using magneto-mechanical coating. J. Sound Vib. 245 (4), 701–714.

Yu, L.M., Ma, Y., Zhou, C.G., Xu, H.B., 2005. The influence of NiCrAlY coatings prepared by LPPS and EB-PVD on the damping properties of 1Cr18Ni9Ti alloy. Mater. Sci. Forum. 475–479, 3971–3976.

Zhang, J.M., Perez, R.J., Wong, C.R. et al., 1994. Effects of secondary phases on the damping behaviour of metals, alloys and metal matrix composites. Mater. Sci. Eng. R 13, 325–390.